

## **Sandwich nanoporous framework decorated with vertical CuO nanowire arrays for electrochemical glucose sensing**

Rui Li<sup>1,2</sup>, Xiongjun Liu<sup>1\*</sup>, Hui Wang<sup>1\*</sup>, Yuan Wu<sup>1</sup>, K. C. Chan<sup>2</sup> and Zhaoping Lu<sup>1</sup>

<sup>1</sup>State Key Laboratory for Advanced Metals and Materials, University of Science and Technology Beijing, Beijing 100083, P. R. China

<sup>2</sup>Advanced Manufacturing Technology Research Centre, Department of Industrial and Systems Engineering, The Hong Kong Polytechnic University, Hong Kong

### **Abstract**

Increasing demands for electrochemical glucose sensors with high overall performance have recently attracted intensive attention. Herein, we report a novel sandwich-like nanoarchitecture composed of uniform CuO nanowire array layers grown on the internal nanoporous Cu<sub>2</sub>O film, which was synthesized via annealing the nanoporous copper thin film obtained by dealloying Cu-based metallic glass precursors. The glucose sensor based on the newly developed CuO/Cu<sub>2</sub>O nanocomposite exhibits prominent overall electrocatalytic performance towards the oxidation of glucose with a wide linear dynamic detection range from 0.1 to 6 mM, high sensitivity up to 1.95 mA/cm<sup>2</sup>·mM, fast response time of less than 1.5 s, low detection limit of 1 μM (S/N=3) as well as excellent selectivity. The enhanced electrocatalytic property of the nanocomposite is attributed to the high surface area originated from the in-situ grown CuO nanowire array structure and synergetic bi-continuous nanoporous Cu<sub>2</sub>O substrate. This finding not only provides promising candidates for blood glucose sensing, but also opens a new avenue to designing nanostructured catalysts for engineering applications in general.

**Keywords:** Nanoporous; CuO nanowire; Dealloying; Glucose sensor; Electrocatalytic activity

\*Corresponding author. Tel. +86 10 82375387; Fax: +86 10 62333447. E-mail: [xjliu@ustb.edu.cn](mailto:xjliu@ustb.edu.cn) or [wanghui@ustb.edu.cn](mailto:wanghui@ustb.edu.cn)

## 1. Introduction

With the increase of the incidence of diabetics over the last decades, novel glucose sensors with improved performance are urgently required. Among various glucose sensors, non-enzymatic electrochemical glucose sensors have attracted extensive attention in the field of medical diagnostics due to their good sensitivity and selectivity as well as long-term stability for non-invasive glucose detection [1-5]. As a result, precious metals or alloys have been extensively explored in the development of electrode materials for non-enzymatic glucose sensors; however, these electrodes are too costly and suffer from the poisoning of intermediates and chloride ions [6-8], which limit their widespread applications. Therefore, development of cost-effective enzyme-free glucose sensors with superior performance is still challenging. Recently, it was found that copper oxides (CuO or Cu<sub>2</sub>O), one kind of *p*-type semiconductors with a narrow band gap, exhibited high catalytic properties in supercapacitors, gas sensors and biosensors [9-13]. Subsequently, possibility of using CuO/Cu<sub>2</sub>O to prepare low cost electrochemical glucose sensors has also been investigated [14-18]. Unfortunately, preliminary results indicate that the overall performances of such sensors in glucose detection need to be further improved.

More recently, it was recognized that catalytic performance of electrochemical glucose sensors is strongly influenced by nanostructure features of electrode materials [19-21]. As a result, a variety of nanostructured CuO/Cu<sub>2</sub>O electrode materials were fabricated in different forms, such as nanowires, nanofibers and nanoflowers, which indeed show meliorated electrocatalytic activities toward the oxidation of glucose [22-

24]. Although various synthesis approaches of CuO/Cu<sub>2</sub>O nanomaterials and many types of CuO/Cu<sub>2</sub>O based electrochemical sensors have been developed, the uncontrollable or non-uniform nanostructure limits their large-scale use in glucose detection [25, 26]. Our previous research reported fabrication of nanoporous copper (NPC) film with well-controlled uniform nanoporosity [27]. However, bare NPC films possess unsatisfactory catalytic activity for the electrocatalytic property towards the oxidation of glucose [28-30]. Considering that NPC films can be oxidized to CuO and/or Cu<sub>2</sub>O directly, we are motivated to develop a quick and easy pathway for fabrication of unique nanoporous thin film decorated with a uniform CuO nanowire array structure by using the free-standing NPC thin film as the precursor.

Herein we report a novel sandwich-like nanocomposite, i.e., vertical CuO nanowire arrays homogeneously grow on both sides of the nanoporous thin film, which can be easily fabricated by heating the as-dealloyed NPC thin film. Such hierarchy nanostructure exhibited promising properties for glucose detection.

## **2. Experimental section**

### **2.1. Synthesis of nanoporous thin film decorated with CuO nanowire arrays**

Glassy precursors with a nominal composition of Cu<sub>60</sub>Zr<sub>35</sub>Al<sub>5</sub> were prepared by melt-spinning under high purity argon atmosphere. The as-spun ribbons which are typically 20-30 μm in thickness and 5-8 mm in width were etched in 0.01 M HF aqueous solution for 24 h at room temperature to fabricate NPC thin film. After being rinsed with ultrapure water and dehydrated alcohol, the cleaned NPC thin films with a

thickness of  $\sim 1.1 \mu\text{m}$  were obtained (see Ref. [27] for details). To fabricate the nanoporous thin film decorated with CuO nanowire array structure, the NPC thin films were heat-treated at  $500 \text{ }^\circ\text{C}$  in air for different annealing durations from 0 to 12 h. After cooling to room temperature, the as-prepared nanostructured thin films were also rinsed with deionized water and dehydrated alcohol.

## 2.2. Microstructure characterization

X-ray diffraction (XRD, Rigaku DMAX-RB-12KW, Cu-K $\alpha$ ) was used to characterize the phases and crystal structures of the samples. Scanning electron microscopy (SEM, Zeiss Supra 55) equipped with an energy dispersive X-ray spectrometer (EDX) and transmission electron microscope (TEM, Tecnai G2 F30) were used to characterize the microstructures of the nanostructured thin films. For the TEM characterization, the thin films were dispersed by sonication in absolute alcohol, and the resultant suspensions were put onto holey carbon-supported copper grids by pipette. The surface chemical state and binding energy of the nanostructured thin films were also investigated by using X-ray photoelectron spectroscopy (XPS AXIS-ULTRA-DLD, Kratos) with an Al K $\alpha$  (mono, 1486.6 eV) anode at an energy of 150 W in a vacuum of  $10^{-7}$  Pa.

## 2.3. Electrochemical measurements of the constructed sensor

All electrochemical measurements were performed in a standard three-electrode system (ACM instrument, GillAC) at room temperature. To evaluate the electrochemical activity of the nanostructured thin film with CuO nanowire arrays, an oxidized nanoporous Cu<sub>2</sub>O thin film without grown nanowires was used as a reference.

In the three-electrode system, a glassy carbon electrode (GCE, 3 mm diameter) modified with nanostructured samples was employed as the working electrode while an Ag-AgCl standard electrode (3 M KCl) was used as the reference electrode and a Pt plate was used as the auxiliary electrode. The supporting electrolyte used for non-enzymatic glucose sensing was 0.1 mol/L NaOH aqueous solution. To prepare the nanostructured thin film modified GCEs, 10  $\mu$ L of 25 g/L as-prepared sample with 0.5 wt.% Nafion solution was dropped onto the polished surface of the GCE. The cyclic voltammograms (CV) of the catalysts were determined in the potential range of 0-0.8 V versus the Ag/AgCl standard reference electrode. The amperometric measurements were conducted by adding different concentrations of glucose consecutively at a fixed potential, and the current at each glucose concentration was recorded after the corresponding steady state was reached.

### 3. Results and discussion

(Fig. 1)

The fabrication procedure of the nanoporous thin film decorated with nanowire arrays is illustrated in **Fig. 1a**, including the chemical dealloying process of Cu-Zr-Al metallic glass and the subsequent thermal oxidation of the dealloyed NPC. The as-spun ribbon exhibits an amorphous structure, and plenty of paralleled shear bands formed on the lateral surface of the fractured ribbon, which is a common feature of deformed MGs (**Fig. 1b**). By utilizing the disparity in chemical stability of the constituent elements, the relatively active Zr and Al were selectively dissolved from the glassy ribbon via chemical dealloying in HF aqueous solutions. **Fig. 1c** presents the cross-sectional image of the dealloyed NPC thin film, which shows a representative morphology of uniform bi-continuous nanoporous structure with interconnected pore channels and Cu ligaments. The pore size of the NPC thin film was measured to be approximately 45 nm. **Fig. 1d** displays the cross-section morphology of a typical as-oxidized thin film heat-treated at 500 °C in air for 4 h. As shown, a sandwich-like structure i.e., a nanoporous region in-between and two outer layers decorated with nanowire arrays with a similar thickness on both surfaces is observed.

(Fig. 2)

Representative XRD spectrums of the as-spun, as-dealloyed and as-oxidized samples are shown in **Fig. 2a**. As can be seen, the as-spun  $\text{Cu}_{60}\text{Zr}_{35}\text{Al}_5$  ribbons possess an amorphous structure, the dealloyed film is face-centered cubic (*fcc*) Cu, but the as-oxidized thin film turns into the CuO and  $\text{Cu}_2\text{O}$  phases. To clarify the distribution of

these phases that formed on the oxidized thin film, SEM observations combined with EDS analyses were carefully conducted. As shown in **Fig. 2c**, the outer layers consisting of nanowire arrays (i.e., Layer i) are identified to be the CuO phase, while the internal nanoporous region (i.e., Layer ii) is determined to be Cu<sub>2</sub>O. These results are in good agreement with the XRD characterization present in **Fig. 2a**.

*(Fig. 3)*

In order to further reveal the formation mechanism of the sandwich-like nanostructure decorated with CuO nanowire arrays, we monitored the surface structural evolution of the nanostructured thin film by tuning the heating treatment time. **Fig. 3** illustrates morphology of the sample surfaces with different thermal oxidation durations ranging from 0 to 12 h. For the dealloyed NPC thin film, the isotropic nanopores and Cu ligaments uniformly distribute in the entire surface (**Fig. 3a**). After being annealed at 500 °C for 1h, the NPC thin film was oxidized, as shown in **Fig. 3b**. It is seen that the thermal oxidation process leads to an obvious coarsening of the nanoporosity, and the nanoporous surface becomes much rougher. The corresponding XRD result indicates that the oxidative product is Cu<sub>2</sub>O. As the heat treatment time increases to 2 h, the Cu<sub>2</sub>O was further oxidized to CuO and a few scattered CuO nanowires began to grow out of the nanoporous surface (**Fig. 3c**). As the oxidation time extends to 3 h, the nanowire array appeared on the surface of sample (**Fig. 3d**). Note that that the all nanowires were grown uniformly in the orientation perpendicular to the nanoporous surface. **Fig. 3e** shows SEM image of the nanowire array structure for the sample annealed for 4 h. In comparison with the CuO nanowire shown in **Fig. 3d**, the entire

surface of this sample is covered by high density of straight nanowires with a longer length and larger diameter. As shown in **Fig. 3f**, however, an unregulated growth of CuO occurred as the heat treatment time prolongs to 12 h. The over-grown CuO nanowires tended to form disordered and agglomerated clusters (the inset in **Fig. 3f**). Based on the above observations, it is known that the formation of CuO nanowire array structure is strongly dependent on heat treatment time and temperature. By adjusting the thermal oxidation time within a proper range at an appropriate temperature, uniform vertical CuO nanowire array structure can be obtained.

*(Fig. 4)*

We further characterized microstructure of the grown CuO nanowire array structure. **Fig. 4a** shows the surface morphology of typical CuO nanowire arrays obtained from the specimen annealed for 4 h. It is seen that a dense array of highly ordered CuO nanowires is uniformly distributed on the surface of the NPC thin film and most of the nanowires grow along the axis direction of the nanoporous surface. The homogeneous distribution of the straight CuO nanowires results from the characteristic nanoporous structure of the NPC precursor. Based on the above results and the findings reported in literature [31-33], we conclude that the formation process of the CuO nanowires includes two reaction steps:



During the initial annealing process, the NPC substrate was firstly oxidized to Cu<sub>2</sub>O, and then the Cu<sub>2</sub>O was further oxidized to CuO and grown into nanowires via the grain-

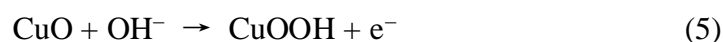
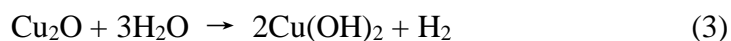
boundary diffusion of Cu ions towards the Cu<sub>2</sub>O/air interface, which usually occurs at the site with a high curvature, such as pores, interfaces and flaws [32, 34]. In our case, growth of the CuO nanowires tends to take place around the uniform nano-pores, thus, a homogeneous nanowire array structure developed. **Fig. 4b** displays a TEM image of the CuO nanowires, indicating a smooth surface of the nanowires. The average diameter of the nanowires was determined to be approximately 120 nm. The HRTEM image exhibits well-defined lattice fringes (**Fig. 4c**), revealing the crystalline nature of the CuO nanowires. The interplanar spacing of the CuO nanowires was measured to be 0.275 nm, which is in good agreement with the (110) plane of the monoclinic CuO. The corresponding fast Fourier transformed (FFT) pattern (the inset in **Fig. 4c**) further confirms that the as-grown CuO nanowires are single crystal in nature with a growth orientation along the axis [100] direction. The surface chemical composition of nanowire arrays was also confirmed by XPS measurements. In the high-resolution XPS spectra of the surface of the as-prepared sample (**Fig. 4d**), two distinct peaks located at 953.9 and 934.2 eV correspond to the binding energy of Cu 2p<sub>1/2</sub> and Cu 2p<sub>3/2</sub> respectively, indicating the presence of the Cu<sup>2+</sup>. In addition, shake-up satellite structures of the 2p<sub>1/2</sub> (centered at 962.7 eV) and 2p<sub>3/2</sub> (centered at 944.8 and 941.7 eV) core lines were also observed, which are typical of Cu<sup>2+</sup> species [35, 36]. No peaks of other elements except C, Cu and O were observed in the whole XPS spectrum of the sample (the inset of **Fig. 4d**), confirming that the grown nanowires are pure CuO.

*(Fig. 5)*

The nanoporous thin film decorated with uniform nanowire arrays was utilized as

catalytically active electrode materials for the oxidation of glucose. For comparison, we also used an oxidized nanoporous  $\text{Cu}_2\text{O}$  thin film without nanowires as a reference. The electrocatalytic properties of the nanoporous thin film decorated with nanowire arrays modified GCE (NP- $\text{Cu}_2\text{O}/\text{CuO}$  NWA/GCE), nanoporous  $\text{Cu}_2\text{O}$  thin film modified GCE (NP- $\text{Cu}_2\text{O}/\text{GCE}$ ), and Nafion/GCE samples were investigated by the CV method in the 0.1 M NaOH aqueous solution at a scan rate of 50 mV/s with/without 1 mM glucose. **Fig. S1** shows the CV curves for the three electrodes in the alkaline blank solution, clearly demonstrating that no obvious current signal is observed for the Nafion/GCE. For the NP- $\text{Cu}_2\text{O}/\text{CuO}$  NWA/GCE and NP- $\text{Cu}_2\text{O}/\text{GCE}$ , the current densities increase distinctly. More importantly, the  $\text{Cu}_2\text{O}/\text{CuO}$  NWA/GCE shows a higher current density than that of the NP- $\text{Cu}_2\text{O}/\text{GCE}$  due to the presence of grown active CuO nanowires. However, the corresponding oxidation peak of Cu(II)/Cu(III) from 0.3 to 0.8 V is not clearly observed at the electrodes, which could be overlaid by the oxidation peak of water-splitting [37, 38]. Upon addition of 1 mM glucose, as shown in **Fig. 5a**, there is still no obvious signal responsible for the electro-oxidation of glucose on the Nafion/GCE, while typical voltammogram with a dramatic increase of current signal is observed for the NP- $\text{Cu}_2\text{O}/\text{CuO}$  NWA/GCE and NP- $\text{Cu}_2\text{O}/\text{GCE}$ . The electro-oxidation process of glucose on the NP- $\text{Cu}_2\text{O}/\text{CuO}$  NWA/GCE and NP- $\text{Cu}_2\text{O}/\text{GCE}$  both starts at around 0.31 V (vs. Ag/AgCl) with an oxidation peak at around 0.58 V (vs. Ag/AgCl), which can be attributed to the transformation of Cu( II ) to Cu(III) under oxidation. In the NaOH solution, the Cu( II ) tends to be electro-oxidized into Cu(III), then the oxidized Cu(III) interact with glucose as an electron-transfer medium

to generate gluconolactone, and finally further oxidized to glucose acid, which can be described by the following reactions [17, 39]:



In comparison with the NP-Cu<sub>2</sub>O/GCE, the NP-Cu<sub>2</sub>O/CuO NWA/GCE exhibits a higher anodic current density, indicating its better catalytic property for the oxidation of glucose. The enhanced electrochemical performance is associated with the high electrocatalytic activity of the in-situ grown CuO nanowires. In this case, the intermediate CuOOH was generated on the surface of the CuO nanowire array structure rapidly and the oxidized glucose is directly converted to gluconolactone as described by Eqs. (5) and (6), leading to the enhancement of the oxidation current density and the decay of reduction current density. **Fig. 5b** exhibits the CV curves of the NP-Cu<sub>2</sub>O/CuO NWA/GCE in the 0.1 M NaOH electrolyte with the presence of various concentrations of glucose. Clearly, the NP-Cu<sub>2</sub>O/CuO NWA/GCE shows no apparent anodic current peak in the absence of glucose, while the anodic current increases gradually as the glucose concentration increase from 1 to 4 mM. The strong independence of current density on glucose concentration indicates a good electrocatalytic activity of the NP-Cu<sub>2</sub>O/CuO NWA/GCE for glucose. Moreover, the scan-rate effects on the oxidation behavior of glucose were also investigated. **Fig. 5c** illustrates the CV responses of NP-Cu<sub>2</sub>O/CuO NWA/GCE in the 0.1 M NaOH solution with 1 mM glucose at the scan rate

from 10 to 200 mV/s. The dependence of current density at 0.58 V (*vs.* Ag/AgCl) on the scan rate is shown in **Fig. 5d**. It is seen that the current density of the anodic oxidation peak of glucose is proportional to the scan rate in a nearly linear relationship with a R-square value of 0.997, suggesting that the electrochemical oxidation is a surface adsorption confined process, where glucose molecules are adsorbed and oxidized on the surface of the NP-Cu<sub>2</sub>O/CuO NWA/GCE [40, 41].

*(Fig. 6)*

*(Table 1)*

To further evaluate the sensitivity and selectivity of the NP-Cu<sub>2</sub>O/CuO NWA towards the glucose oxidation, amperometric experiments of the NP-Cu<sub>2</sub>O/CuO NWA/GCE were also performed. For the amperometric experiments, the potential of oxidation peak at 0.58 V (*vs.* Ag/AgCl) was selected as the sensing voltage. **Fig. 6a** shows a typical amperometric curve of the NP-Cu<sub>2</sub>O/CuO NWA/GCE with successive additions of different concentration glucose into the 0.1 M NaOH at 0.58 V (*vs.* Ag/AgCl). As can be seen, the NP-Cu<sub>2</sub>O/CuO NWA/GCE exhibits a rapid amperometric response for addition of glucose, and the time required to reach the stable response is ~1.5 s, which is defined as the time for the current density to reach the steady-state value. This value is much smaller than those of recent reported electrodes, such as CuO/Cu<sub>2</sub>O nanosheets (~3 s) [17], and Nanoporous CuO/Cu (~2 s) [42]. As shown in the magnified view of the amperometric response at low concentration of glucose (i.e., the inset in **Fig. 6a**), the detection limit is around 1 μM (S/N=3), lower than that of the reported bare CuO nanowire electrode (2 μM) [43]. The extended

detection range may be due to the fact that the 3D bi-continuous nanoporous structure of the NP-Cu<sub>2</sub>O/CuO NWA possesses a larger specific surface area which provides more effective contact between the electrolyte and nanostructured CuO/Cu<sub>2</sub>O catalysts. Note that this critical value is also far below the physiological blood glucose level (3~8 mM), demonstrating excellent detecting capability of the NP-Cu<sub>2</sub>O/CuO NWA/GCE. For comparison, current density-concentration calibration curves of the NP-Cu<sub>2</sub>O/CuO NWA/GCE and NP-Cu<sub>2</sub>O/GCE are presented in **Fig. 6b**, and from which the sensitivity is determined to be ~1.95 mA/cm<sup>2</sup>·mM while the detection range is from 0.1 to 6 mM for the NP-Cu<sub>2</sub>O/CuO NWA/GCE. The corresponding values for the NP-Cu<sub>2</sub>O/GCE are ~1.45 mA/cm<sup>2</sup>·mM and 4 mM, respectively, indicating that NP-Cu<sub>2</sub>O/CuO NWA/GCE has higher sensitivity in the detection of glucose than that of the NP-Cu<sub>2</sub>O/GCE. In addition, the sensitivity of our nanostructured sandwich electrode is also much higher than that of recent reported nanoporous copper/carbon [44], Cu@Cu<sub>2</sub>O/rGO [45], and CuO nanoparticles [13]. **Table 1** further summaries the critical parameters for the glucose sensors based on the present NP-Cu<sub>2</sub>O/CuO NWA/GCE, in comparison with previously reported electrochemical sensors based on copper, copper oxide or copper hydroxide. Apparently, the NP-Cu<sub>2</sub>O/CuO NWA/GCE possesses a unique combination of sensing properties. The superior electrochemical properties of our sensors in monitoring glucose can be attributed to their novel sandwich nano-architecture and synergistic bi-continuous nanoporous Cu<sub>2</sub>O framework. This nanocomposite structure with a large specific surface area can facilitate sufficient use of the highly active CuO/Cu<sub>2</sub>O and thus allow the developed electrode to detect glucose

at low concentration with high sensitivity. It is known that glucose detections usually suffer from the interfering compounds in physiological environments. Therefore, good anti-interference property is also required for an electrochemical non-enzymatic glucose sensor. In this regard, selectivity tests were performed to investigate the effect of interfering reagents including ascorbic acid (AA), uric acid (UA) and acetaminophen (AP) on the glucose detection of the NP-Cu<sub>2</sub>O/CuO NWA/GCE. **Fig. 6c** shows the current response of the NP-Cu<sub>2</sub>O/CuO NWA/GCE and Nafion/GCE conducted by adding 0.1 mM AA, 0.3 mM UA, 0.1 mM AP and 1 mM glucose in the 0.1 M NaOH electrolyte at 0.58 V (*vs.* Ag/AgCl), respectively. It is found that the addition of AA, UA and AP induce no obvious current density changes for the NP-Cu<sub>2</sub>O/CuO NWA/GCE, whereas that of 1mM glucose results in a quick and significant increase of the current density. In contrast, no noticeable current density increases for the Nafion/GCE when each analyst was added. Similar results were also obtained when adding 0.1 mM dopamine (DA) or sugars including 0.1 mM lactose, sucrose, maltose, and fructose in the same NaOH aqueous electrolyte (**Fig. S2**), this finding vividly verifies the good selectivity of the NP-Cu<sub>2</sub>O/CuO NWA/GCE electrode towards glucose detection. Considering the fact that the normal physiological level of glucose is in the range of 3 to 8 mM and the concentrations of the tested interfering substances in human serum are far below, the present NP-Cu<sub>2</sub>O/CuO NWA/GCE exhibits a reliable selectivity towards the oxidation of glucose and is a promising electrode material for applying in human blood glucose detection. Furthermore, stability and reproducibility of the electrode materials are also important for their practical application. In this work,

the stability of the sensor is characterized by the decay of current signal with time during detecting the oxidation of glucose. Note that the current intensity measured at different time periods was normalized with the initial value determined by the first measurement. Then, the long-term stability of the product was monitored by storing the modified electrode in air under ambient environmental conditions and intermittently (every day) measuring the current response. As is shown in **Fig. 6d**, after the durability test of two weeks, the final response remains ~94% of the original amperometric response, indicating that the present electrode is viable for long-term routine services. To evaluate the reproducibility of the present sensor, three prepared electrodes were investigated to compare their amperometric responses toward glucose oxidation, and the relative standard deviation (RSD) was determined to be 3.4 %. In addition, ten measurements of glucose on the same NP-Cu<sub>2</sub>O/CuO NWA/GCE showed an RSD value of 2.6 %. The low RSD values confirm the good reproducibility of our sensor. The long-term stability and good reproducibility of the NP-Cu<sub>2</sub>O/CuO NWA/GCE are probably related to the chemical durability of CuO and Cu<sub>2</sub>O in the NaOH solution and the structure stability of the nanoporosity decorated with uniform nanowire arrays.

*(Table 2)*

To verify the commercialization possibility of newly developed electrodes, the sensor was also used for analyzing the glucose concentration in real human serum. **Fig. S3** presents the amperometric response for the successive additions of 10  $\mu$ L glucose solution (4 mM) and two 10  $\mu$ L blood serum samples into 10 mL of 0.1 M NaOH electrolyte. As expected, the measured glucose concentrations of the blood serum

samples are in good agreement with the given value of the automatic biochemical analyzer used widely in hospital (**Table 2**). The RSD and bias are less than 3 % and 0.15 mM, respectively. This observation further confirms that our sensors are promising for human blood glucose detection.

#### **4. Conclusions**

In summary, by chemical dealloying of Cu-based MG ribbon and the subsequent thermal oxidation treatment of the as-dealloyed NPC, we have developed a novel sandwich-like nanoporous framework decorated with vertical CuO nanowire arrays. The newly developed sensor exhibited superior electrocatalytic performance towards the oxidation of glucose: high sensitivity of  $1.95 \text{ mA/cm}^2 \cdot \text{mM}$ , wide linear dynamic ranges from 0.1 to 6 mM, low detection limit of  $1 \text{ } \mu\text{M}$  ( $S/N=3$ ) and fast response time of 1.5 s, along with good selectivity and long-term stability. The impressive glucose sensing property of the electrode can be attributed to the enhanced electrocatalytic activity of the CuO/Cu<sub>2</sub>O nanocomposite and the high specific surface area benefitted from the unique in-situ grown CuO nanowire array structure and synergetic nanoporous Cu<sub>2</sub>O framework. Our finding has important implications for designing enhanced nanostructured electrocatalysts for engineering applications. To further improve the sensitivity and detection limit, the future work is to promote the electron transportation during glucose oxidation process by adding more conductive supports to the sensor.

## **Acknowledgements**

This research was supported by National Natural Science Foundation of China (Nos. 51871016, 51671018, 11790293, 51531001 and 51671021), 111 Project (B07003), Program for Changjiang Scholars and Innovative Research Team in University of China (IRT\_14R05) and the Projects of SKLAMM-USTB (2018Z-01, 2018Z-19). YW acknowledges the financial support from the Top-Notch Young Talents Program. YW and HW acknowledges the financial support from the Fundamental Research Funds for the Central Universities (No. FRF-TP-15-004C1, FRF-TP-18-004C1).

## References

- [1] C. Chen, Q. Xie, D. Yang, H. Xiao, Y. Fu, Y. Tan, S. Yao, Recent advances in electrochemical glucose biosensors: a review, *Rsc Adv.* 3 (2013) 4473-4491.
- [2] A. Heller, B. Feldman, Electrochemical glucose sensors and their applications in diabetes management, *Chem. Rev.* 108 (2008) 2482-2505.
- [3] P. Si, Y. Huang, T. Wang, J. Ma, Nanomaterials for electrochemical non-enzymatic glucose biosensors, *Rsc Adv.* 3 (2013) 3487-3502.
- [4] A. Weremfo, S.T.C. Fong, A. Khan, D.B. Hibbert, C. Zhao, Electrochemically roughened nanoporous platinum electrodes for non-enzymatic glucose sensors, *Electrochim. Acta* 231 (2017) 20-26.
- [5] C.-L. Hsu, J.-H. Lin, D.-X. Hsu, S.-H. Wang, S.-Y. Lin, T.-J. Hsueh, Enhanced non-enzymatic glucose biosensor of ZnO nanowires via decorated Pt nanoparticles and illuminated with UV/green light emitting diodes, *Sensor Actuat. B-Chem.* 238 (2017) 150-159.
- [6] C. Li, H. Wang, Y. Yamauchi, Electrochemical deposition of mesoporous Pt-Au alloy films in aqueous surfactant solutions: towards a highly sensitive amperometric glucose sensor, *Chem. Eur. J.* 19 (2013) 2242-2246.
- [7] G.-h. Wu, X.-h. Song, Y.-f. Wu, X.-m. Chen, F. Luo, X. Chen, Non-enzymatic electrochemical glucose sensor based on platinum nanoflowers supported on graphene oxide, *Talanta* 105 (2013) 379-385.
- [8] X. Niu, L. Shi, H. Zhao, M. Lan, Advanced strategies for improving the analytical performance of Pt-based nonenzymatic electrochemical glucose sensors: a minireview, *Anal. Methods* 8 (2016) 1755-1764.

- [9] D.P. Dubal, G.S. Gund, R. Holze, C.D. Lokhande, Mild chemical strategy to grow micro-roses and micro-woolen like arranged CuO nanosheets for high performance supercapacitors, *J. Power Sources* 242 (2013) 687-698.
- [10] M. Kuang, T.T. Li, H. Chen, S.M. Zhang, L.L. Zhang, Y.X. Zhang, Hierarchical Cu<sub>2</sub>O/CuO/Co<sub>3</sub>O<sub>4</sub> core-shell nanowires: synthesis and electrochemical properties, *Nanotechnology* 26 (2015) 304002.
- [11] S.A. Zaidi, J.H. Shin, Recent developments in nanostructure based electrochemical glucose sensors, *Talanta* 149 (2016) 30-42.
- [12] K. Ghanbari, Z. Babaei, Fabrication and characterization of non-enzymatic glucose sensor based on ternary NiO/CuO/polyaniline nanocomposite, *Anal. Biochem.* 498 (2016) 37-46.
- [13] Y. Zhong, T. Shi, Z. Liu, S. Cheng, Y. Huang, X. Tao, G. Liao, Z. Tang, Ultrasensitive non-enzymatic glucose sensors based on different copper oxide nanostructures by in-situ growth, *Sensor Actuat. B-Chem.* 236 (2016) 326-333.
- [14] X. Wang, C. Hu, H. Liu, G. Du, X. He, Y. Xi, Synthesis of CuO nanostructures and their application for nonenzymatic glucose sensing, *Sensor Actuat. B-Chem.* 144 (2010) 220-225.
- [15] S. Felix, P. Kollu, B.P. Raghupathy, S.K. Jeong, A.N. Grace, Electrocatalytic activity of Cu<sub>2</sub>O nanocubes based electrode for glucose oxidation, *J. Chem. Sci.* 126 (2014) 25-32.
- [16] D. Chirizzi, M.R. Guascito, E. Filippo, C. Malitesta, A. Tepore, A novel nonenzymatic amperometric hydrogen peroxide sensor based on CuO@Cu<sub>2</sub>O

- nanowires embedded into poly (vinyl alcohol), *Talanta* 147 (2016) 124-131.
- [17] J. Lv, C. Kong, Y. Xu, Z. Yang, X. Zhang, S. Yang, G. Meng, J. Bi, J. Li, S. Yang, Facile synthesis of novel CuO/Cu<sub>2</sub>O nanosheets on copper foil for high sensitive nonenzymatic glucose biosensor, *Sensor Actuat. B-Chem.* 248 (2017) 630-638.
- [18] L.-Y. Lin, B.B. Karakocak, S. Kavadiya, T. Soundappan, P. Biswas, A highly sensitive non-enzymatic glucose sensor based on Cu/Cu<sub>2</sub>O/CuO ternary composite hollow spheres prepared in a furnace aerosol reactor, *Sensor Actuat. B-Chem.* 259 (2018) 745-752.
- [19] J. Xiang, J. Tu, L. Zhang, Y. Zhou, X. Wang, S. Shi, Self-assembled synthesis of hierarchical nanostructured CuO with various morphologies and their application as anodes for lithium ion batteries, *J. Power Sources* 195 (2010) 313-319.
- [20] H. Mistry, A.S. Varela, S. Kuehl, P. Strasser, B.R. Cuenya, Nanostructured electrocatalysts with tunable activity and selectivity, *Nat. Rev. Mater.* 1 (2016) 16009.
- [21] M. Kuang, G. Zheng, Nanostructured bifunctional redox electrocatalysts, *Small* 12 (2016) 5656-5675.
- [22] B. Zheng, G. Liu, A. Yao, Y. Xiao, J. Du, Y. Guo, D. Xiao, Q. Hu, M.M. Choi, A sensitive AgNPs/CuO nanofibers non-enzymatic glucose sensor based on electrospinning technology, *Sensor Actuat. B-Chem.* 195 (2014) 431-438.
- [23] S. Sun, X. Zhang, Y. Sun, S. Yang, X. Song, Z. Yang, Hierarchical CuO nanoflowers: water-required synthesis and their application in a nonenzymatic glucose biosensor, *Phys. Chem. Chem. Phys.* 15 (2013) 10904-10913.
- [24] X. Liu, W. Yang, L. Chen, J. Jia, Three-dimensional copper foam supported CuO

nanowire arrays: an efficient non-enzymatic glucose sensor, *Electrochim. Acta* 235 (2017) 519-526.

[25] Q. Zhang, K. Zhang, D. Xu, G. Yang, H. Huang, F. Nie, C. Liu, S. Yang, CuO nanostructures: synthesis, characterization, growth mechanisms, fundamental properties, and applications, *Prog. Mater. Sci.* 60 (2014) 208-337.

[26] Y. Qian, F. Ye, J. Xu, Z.-G. Le, Synthesis of cuprous oxide (Cu<sub>2</sub>O) nanoparticles/graphene composite with an excellent electrocatalytic activity towards glucose, *Int. J. Electrochem. Sci.* 7 (2012) 10063-10073.

[27] R. Li, X. Liu, H. Wang, Y. Wu, Z. Lu, Bendable nanoporous copper thin films with tunable thickness and pore features, *Corros. Sci.* 104 (2016) 227-235.

[28] S. Sattayasamitsathit, P. Thavarungkul, C. Thammakhet, W. Limbut, A. Numnuam, C. Buranachai, P. Kanatharana, Fabrication of nanoporous copper film for electrochemical detection of glucose, *Electroanal.* 21 (2009) 2371-2377.

[29] G. Wang, X. He, L. Wang, A. Gu, Y. Huang, B. Fang, B. Geng, X. Zhang, Non-enzymatic electrochemical sensing of glucose, *Microchim. Acta* 180 (2013) 161-186.

[30] Y. Zhao, L. Fan, Y. Zhang, H. Zhao, X. Li, Y. Li, L. Wen, Z. Yan, Z. Huo, Hyper-Branched Cu@Cu<sub>2</sub>O Coaxial Nanowires Mesh Electrode for Ultra-Sensitive Glucose Detection, *ACS Appl. Mater. Inter.* 7 (2015) 16802-16812.

[31] S.-L. Cheng, M.-F. Chen, Fabrication, characterization, and kinetic study of vertical single-crystalline CuO nanowires on Si substrates, *Nanoscale Res. Lett.* 7 (2012) 119.

[32] M. Zhong, D. Zeng, Z. Liu, H. Yu, X. Zhong, W. Qiu, Synthesis, growth

mechanism and gas-sensing properties of large-scale CuO nanowires, *Acta Mater.* 58 (2010) 5926-5932.

[33] M. Zheng, D. Yu, L. Duan, W. Yu, L. Huang, In-situ fabricated CuO nanowires/Cu foam as a monolithic catalyst for plasma-catalytic oxidation of toluene, *Catal. Commun.* 100 (2017) 187-190.

[34] J. Li, J. Mayer, E. Colgan, Oxidation and protection in copper and copper alloy thin films, *J. Appl. Phys.* 70 (1991) 2820-2827.

[35] J. Ghijsen, L. Tjeng, J. Van Elp, H. Eskes, J. Westerink, G. Sawatzky, M. Czyzyk, Electronic structure of Cu<sub>2</sub>O and CuO, *Phys. Rev. B* 38 (1988) 11322.

[36] R. Li, K. Chan, X. Liu, X. Zhang, L. Liu, T. Li, Z. Lu, Synthesis of well-aligned CuO nanowire array integrated with nanoporous CuO network for oxidative degradation of methylene blue, *Corros. Sci.* 126 (2017) 37-43.

[37] L.-C. Jiang, W.-D. Zhang, A highly sensitive nonenzymatic glucose sensor based on CuO nanoparticles-modified carbon nanotube electrode, *Biosens. Bioelectron.* 25 (2010) 1402-1407.

[38] X. Liu, S. Cui, Z. Sun, P. Du, Copper oxide nanomaterials synthesized from simple copper salts as active catalysts for electrocatalytic water oxidation, *Electrochim. Acta* 160 (2015) 202-208.

[39] J. Huang, Y. Zhu, X. Yang, W. Chen, Y. Zhou, C. Li, Flexible 3D porous CuO nanowire arrays for enzymeless glucose sensing: in situ engineered versus ex situ piled, *Nanoscale* 7 (2015) 559-569.

[40] S.G. Leonardi, S. Marini, C. Espro, A. Bonavita, S. Galvagno, G. Neri, In-situ

grown flower-like nanostructured CuO on screen printed carbon electrodes for non-enzymatic amperometric sensing of glucose, *Microchim. Acta* 184 (2017) 2375-2385.

[41] W. Zhang, R. Li, L. Xing, X. Wang, X. Gou, Carnatio-like CuO hierarchical nanostructures assembled by porous nanosheets for nonenzymatic glucose sensing, *Electroanal.* 28 (2016) 2214-2221.

[42] C. Li, M. Kurniawan, D. Sun, H. Tabata, J.-J. Delaunay, Nanoporous CuO layer modified Cu electrode for high performance enzymatic and non-enzymatic glucose sensing, *Nanotechnology* 26 (2014) 015503.

[43] Y. Zhang, Y. Liu, L. Su, Z. Zhang, D. Huo, C. Hou, Y. Lei, CuO nanowires based sensitive and selective non-enzymatic glucose detection, *Sensor Actuat. B-Chem.* 191 (2014) 86-93.

[44] L. Mei, P. Zhang, J. Chen, D. Chen, Y. Quan, N. Gu, G. Zhang, R. Cui, Non-enzymatic sensing of glucose and hydrogen peroxide using a glassy carbon electrode modified with a nanocomposite consisting of nanoporous copper, carbon black and nafion, *Microchim. Acta* 183 (2016) 1359-1365.

[45] H. Huo, C. Guo, G. Li, X. Han, C. Xu, Reticular-vein-like Cu@Cu<sub>2</sub>O/reduced graphene oxide nanocomposites for a non-enzymatic glucose sensor, *Rsc Adv.* 4 (2014) 20459-20465.

[46] C. Kong, L. Tang, X. Zhang, S. Sun, S. Yang, X. Song, Z. Yang, Templating synthesis of hollow CuO polyhedron and its application for nonenzymatic glucose detection, *J. Mater. Chem. A* 2 (2014) 7306-7312.

[47] J. Yang, L.-C. Jiang, W.-D. Zhang, S. Gunasekaran, A highly sensitive non-

enzymatic glucose sensor based on a simple two-step electrodeposition of cupric oxide (CuO) nanoparticles onto multi-walled carbon nanotube arrays, *Talanta* 82 (2010) 25-33.

[48] L. Ju, G. Wu, B. Lu, X. Li, H. Wu, A. Liu, Non-enzymatic amperometric glucose sensor based on copper nanowires decorated reduced graphene oxide, *Electroanal.* 28 (2016) 2543-2551.

[49] I. Shackery, U. Patil, A. Pezeshki, N.M. Shinde, S. Kang, S. Im, S.C. Jun, Copper hydroxide nanorods decorated porous graphene foam electrodes for non-enzymatic glucose sensing, *Electrochim. Acta* 191 (2016) 954-961.

[50] X. Xiao, H. Li, Y. Pan, P. Si, Non-enzymatic glucose sensors based on controllable nanoporous gold/copper oxide nanohybrids, *Talanta* 125 (2014) 366-371.

## Figure and Table captions

**Fig. 1.** (a) Schematic diagram of the synthesis process of the nanoporous thin film decorated with nanowire arrays. Fracture morphologies of the samples: (b) melt-spun  $\text{Cu}_{60}\text{Zr}_{35}\text{Al}_5$  glassy precursor, (c) as-dealloyed NPC thin film, and (d) as-prepared nanoporous thin film decorated with CuO nanowire array structure.

**Fig. 2.** (a) XRD patterns of the as-spun  $\text{Cu}_{60}\text{Zr}_{35}\text{Al}_5$  ribbon, dealloyed NPC thin film and oxidized nanostructured thin film. (b) High magnification cross-sectional SEM image of the oxidized thin film and (c) EDS spectra taken from the layers marked as (i) and (ii) shown in (b).

**Fig. 3.** Surface morphology of nanostructured thin film prepared after different annealing durations: (a) 0 h (bare NPC), (b) 1 h, (c) 2 h, (d) 3 h, (e) 4 h and (f) 12 h. The inset is a SEM morphology of the sample annealed for 12 h in a low magnification.

**Fig. 4.** (a) SEM characterization of nanoporous thin film obtained after 4 h annealing. (b) TEM image of the as-grown CuO nanowires. (c) HRTEM image of the CuO nanowire. The inset shows the corresponding fast Fourier transformed (FFT) pattern. (d) High-resolution XPS spectra of Cu 2p of the surface of the sample. The inset shows an overall XPS spectra.

**Fig. 5.** (a) CV curves for the NP-Cu<sub>2</sub>O/CuO NWA/GCE, NP-Cu<sub>2</sub>O/GCE and

Nafion/GCE in the 0.1 M NaOH electrolyte with presence of 1 mM glucose at a scan rate of 50 mV/s. (2) CV curves for the NP-Cu<sub>2</sub>O/CuO NWA/GCE in various glucose concentrations ranging from 0 to 4 mM. (c) CV curves on NP-Cu<sub>2</sub>O/CuO NWA/GCE in the 1.0 M NaOH electrolyte with presence of 1 mM glucose at different scan rates ranging from 10 to 200 mV/s. (d) The calibration curve of the oxidative peak current density vs scan rate.

**Fig. 6.** (a) Amperometric responses of the NP-Cu<sub>2</sub>O/CuO NWA/GCE with successive addition of different concentration glucoses to the 0.1 M NaOH electrolyte at 0.58 V (vs. Ag/AgCl). The inset is the enlarged amperometric responses with low glucose concentration. (b) Current density-glucose concentration calibration plots for the NP-Cu<sub>2</sub>O/CuO NWA/GCE and NP-Cu<sub>2</sub>O/GCE. (c) Anti-interference performance of the NP-Cu<sub>2</sub>O/CuO NWA/GCE with addition of 0.1 mM AA, 0.3 mM UA, 0.1 mM AP and 1 mM glucose in the 0.1 M NaOH electrolyte at 0.58 V (vs. Ag/AgCl), respectively. (d) Long-term stability test of the NP-Cu<sub>2</sub>O/CuO NWA/GCE for 2 weeks.

**Table 1.** Performance of the currently developed glucose sensor in comparison with that of various reported glucose sensors based on copper, copper oxide and copper hydroxide.

**Table 2.** Comparison of glucose concentrations of human blood serum samples measured by automatic biochemical analyzer (Olympus AU400) and our NP-Cu<sub>2</sub>O/CuO NWA/GCE sensor.

Fig. 1 by Li et al.

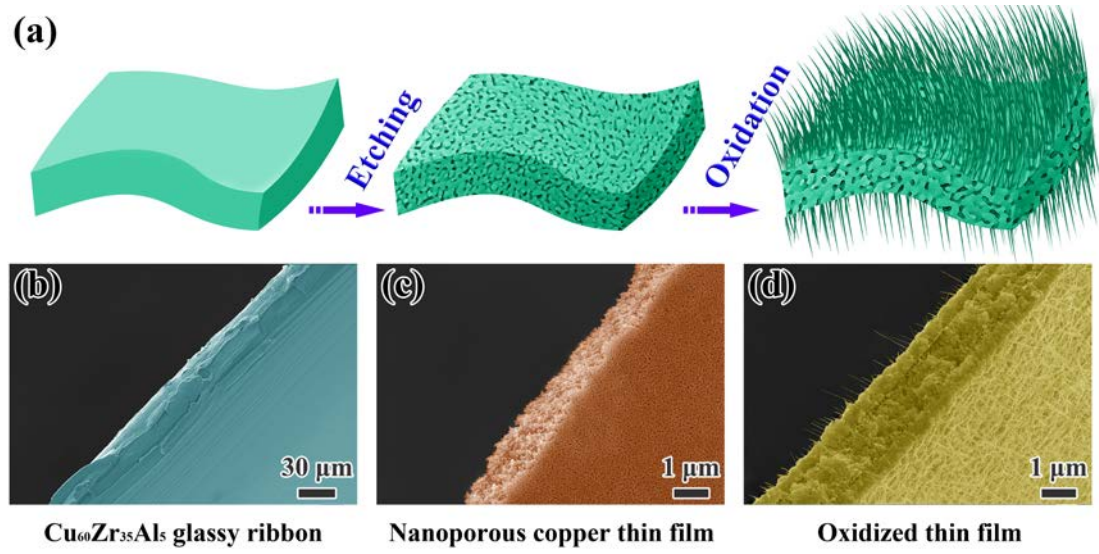


Fig. 2 by Li et al.

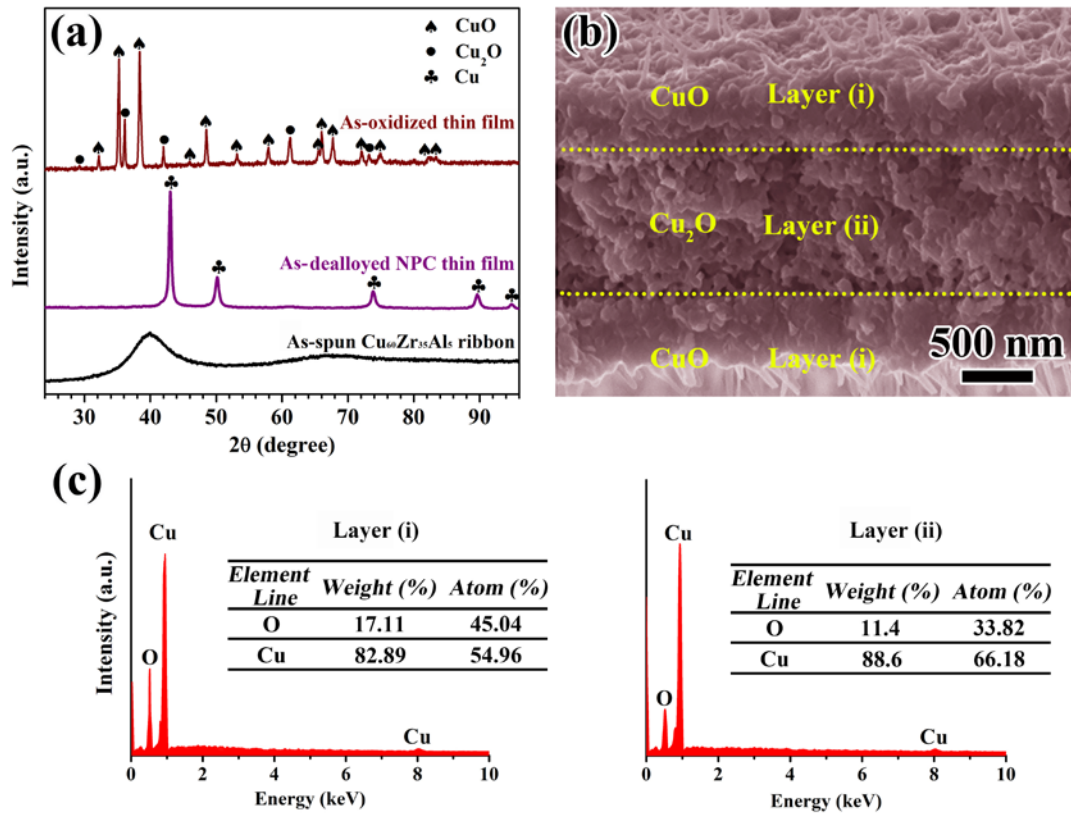


Fig. 3 by Li et al.

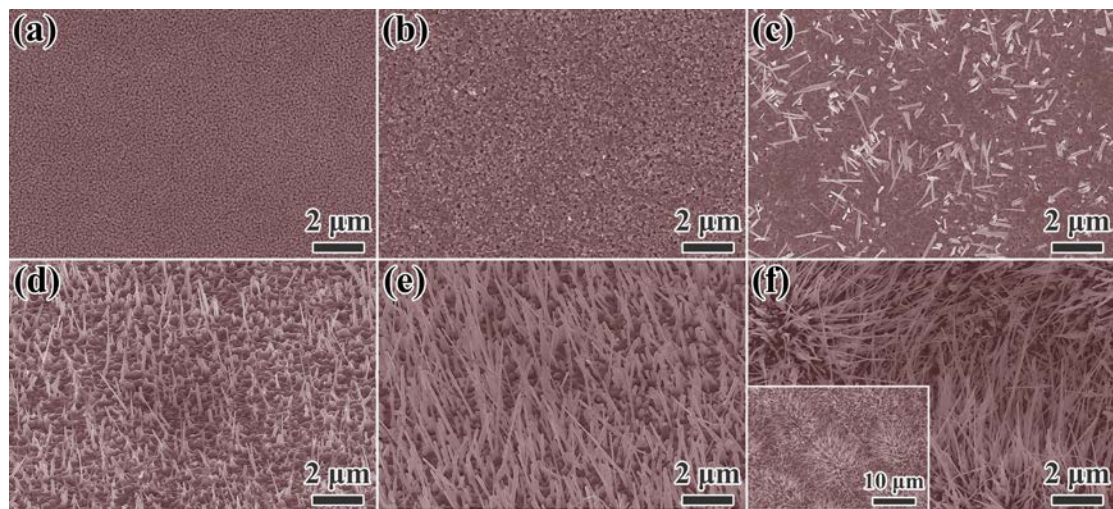


Fig. 4 by Li et al.

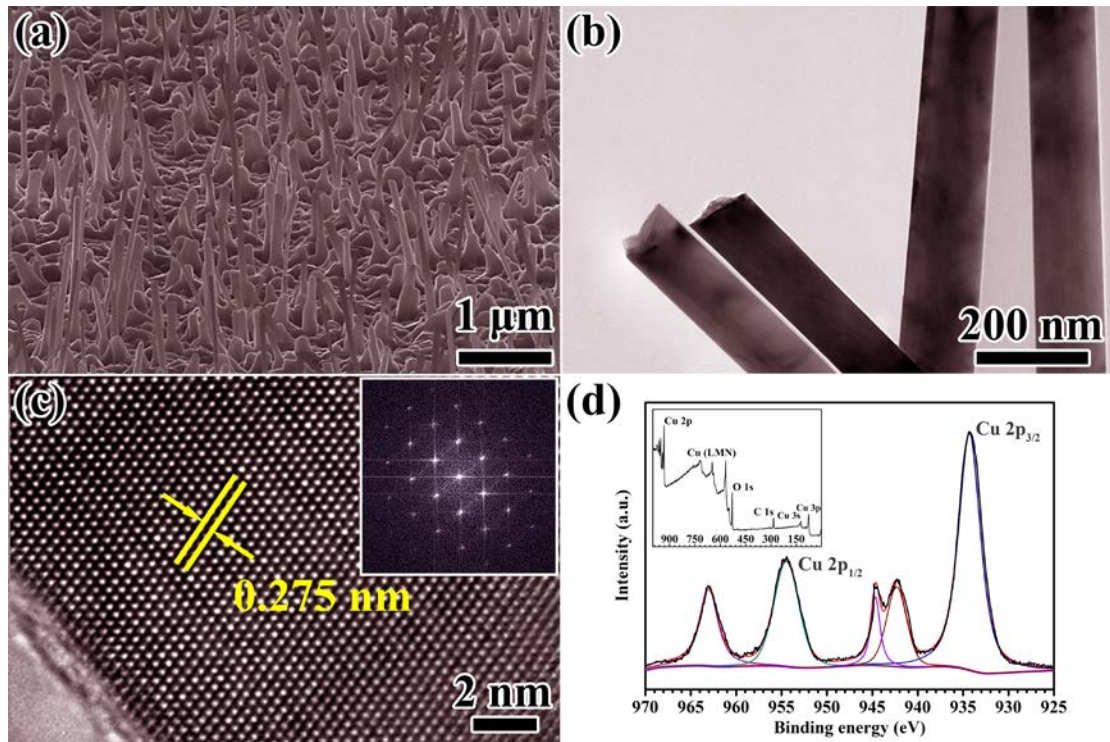


Fig. 5 by Li et al.

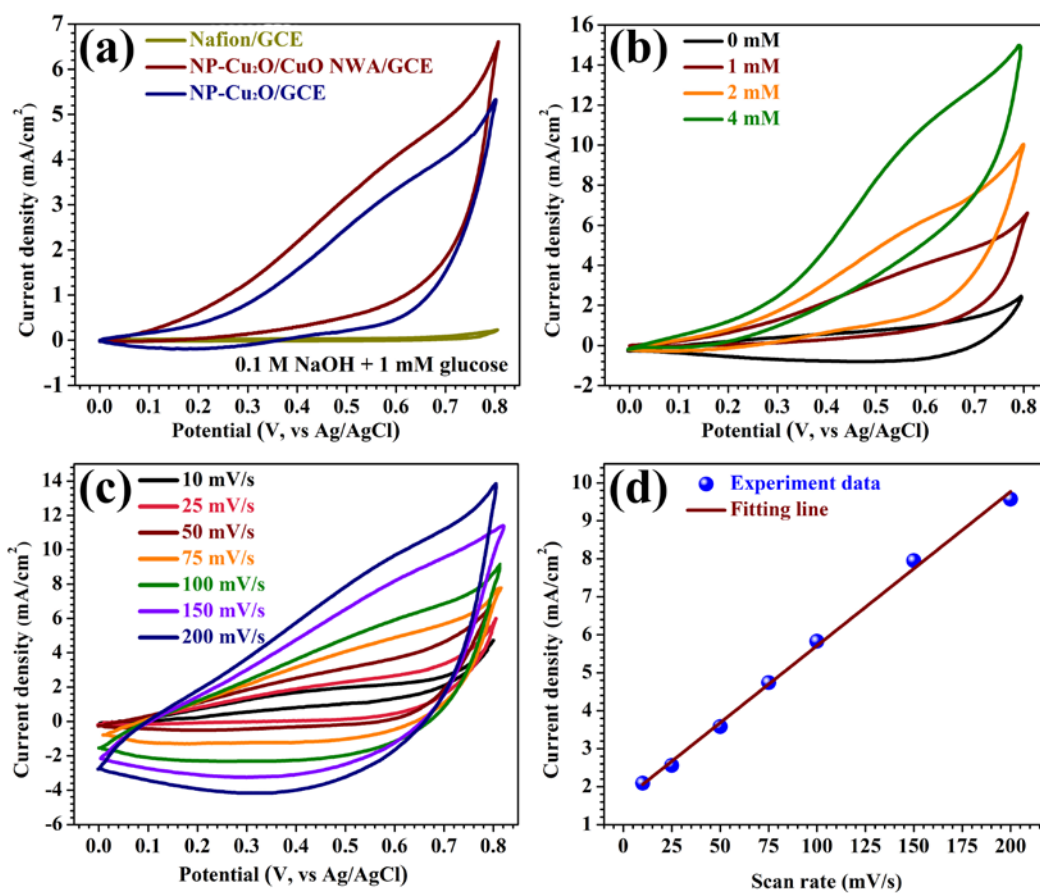
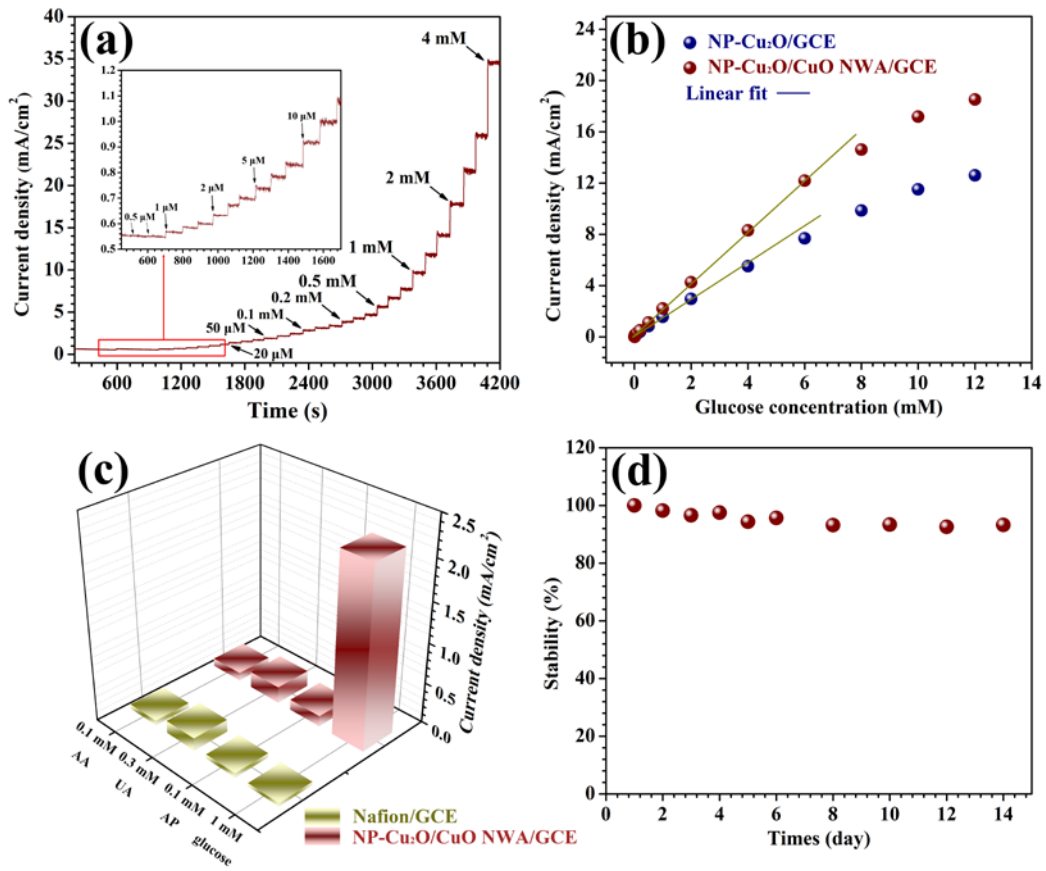


Fig. 6 by Li et al.



**Table 1 by Li et al.**

Electrode materials	Potential (V)	Sensitivity (mA/cm <sup>2</sup> .mM)	Linear range (mM)	Detection limit (μM)	Ref.
<b>NP-Cu<sub>2</sub>O/CuO NWA/GCE</b>	<b>0.58</b>	<b>1.95</b>	<b>0.1 to 6</b>	<b>1</b>	<b>Our work</b>
CuO nanowires/GCE	0.55	0.65	-	2	[43]
CuO nanoparticle /Carbon cloth	0.55	1.24	Up to 1.25	1	[13]
Hollow CuO polyhedron/GCE	0.55	1.11	Up to 4	0.33	[46]
CuO nanowire/Cu foil	0.35	1.42	Up to 2.55	5.1	[39]
CuO/MWCNT/GCE	0.7	2.1	Up to 3	0.8	[47]
CuO/Cu <sub>2</sub> O nanosheets @Copper foil	0.6	1.54	4	0.57	[17]
Cu nanowires @graphene/ITO	0.58	1.63	Up to 11	0.2	[48]
Cu(OH) <sub>2</sub> /graphene	0.6	3.36	1.2×10 <sup>-3</sup> to 6	1.2	[49]
CuO nanoflower /Carbon electrode	0.6	1.46	0.04 to 2	2.5	[40]
NPG/CuO	0.4	0.37	Up to 12	2.8	[50]

**Table 2 by Li et al.**

Sample No.	Automatic biochemical analyzer (mM)	Our Cu <sub>2</sub> O/CuO NWA/GCE (mM)	RSD (%)	Bias (mM)
1	4.6	4.46	3.2	-0.14
2	6.0	5.89	3.9	-0.11

RSD (%) was calculated from three separate measurements.